

## Magma degassing and intermittent lava dome growth

B. Taisne<sup>1</sup> and C. Jaupart<sup>1</sup>

Received 22 July 2008; revised 22 September 2008; accepted 26 September 2008; published 28 October 2008.

[1] After its 1980 explosive eruption, Mount St Helens developed a lava dome that grew intermittently for several years. Each growth episode was followed by a long repose, suggesting that the magma column above the reservoir was in hydrostatic equilibrium. A mechanism allowing an increasingly thicker dome is proposed. Loading of the crater floor by the dome acts to prevent gas leakage from magma by closing fractures around the volcanic conduit. Fractures get closed down to a depth that increases as the dome grows. Calculations of dome thickness as a function of dome radius are in good agreement with observations. Renewed growth is triggered by the spreading of the dome. Gas retention over a larger depth extent allows smaller magma densities and a taller magma column above the reservoir. According to this model, small domes can in fact promote explosive volcanic conditions and be unstable. **Citation:** Taisne, B., and C. Jaupart (2008), Magma degassing and intermittent lava dome growth, *Geophys. Res. Lett.*, 35, L20310, doi:10.1029/2008GL035432.

### 1. Introduction

[2] The 1980–1989 eruption of Mount St Helens (MSH) ended with the slow effusion of gas-poor lava accumulating in a dome. In this waning phase, eruption rates were much slower than in the initial explosive phases. Dome growth proceeded through a series of individual episodes typically lasting a few days separated by longer repose periods.

[3] Several models have been put forward to explain intermittent dome growth. Fluctuations of eruption rate can be generated because of kinetically-controlled crystallization during ascent [Melnik and Sparks, 1999]. They may also arise because of the coupling between pressure in the magma reservoir and the eruption rate of crystallizing magma [Melnik and Sparks, 2005] or because of deformation of the conduit walls [Costa et al., 2007]. These models, however, do not account for dome growth and the implied pressure changes. Another possibility is that degassing paths get sealed by mineral precipitation, leading to gas retention and eventually to explosion and dome destruction [Matthews et al., 1997]. Because of dome destruction, the magma/lava column and the reservoir are no longer in hydrostatic equilibrium, which triggers renewed magma flow in the conduit. At MSH, however, there was no significant destruction save for the first two episodes of June and August 1980. In yet another model, swelling of the dome due to the intrusion of new magma or the expansion of magmatic gases proceeds until failure of the dome carapace [Iverson, 1990].

This model does not specify what stops magma ascent at the end of a growth phase. At MSH, swelling was short-lived and immediately preceded extrusion after a lengthy repose. There was abundant evidence that the carapace allowed degassing: repose periods were punctuated by small gas explosions and the jetting of gas through open fissures. Thus, swelling was due to the supply of new magma and intermittent dome growth reflected intermittent magma ascent.

[4] There can be no doubt that the various processes invoked above do exist, but they do not explain why successive growth episodes lead to a taller dome. Here, we propose a new model that relies on three observations. One is that the height and diameter of the dome increased continuously. The height to diameter ratio was always smaller than the angle of repose for fractured material and changed with time [Swanson and Holcomb, 1990], showing that the shape of the dome was not determined by static equilibrium conditions. Another important fact is that successive growth episodes were separated by long repose periods with no magma flow in the conduit. A third piece of evidence is the gradual long-term decrease of eruption rate. Dome growth is self-defeating because the weight of the magma/lava column increases until it balances the reservoir pressure. This has been successfully tested in several eruptions [Huppert et al., 1982; Jaupart and Allègre, 1991; Stasiuk et al., 1993]. Renewed magma ascent, therefore, requires either an increase of reservoir pressure or a decrease of the weight of the magma/lava column. At MSH, the overall trend of decreasing eruption rate provides no support for an increase of reservoir pressure. For magma that has nearly constant composition and starting volatile content, changes of the weight of the lava column can only come from modifications of exsolved gas content and/or of dome height. We thus focus on changes of degassing conditions due to loading by the dome and on constraints brought by the dome dimensions. The MSH dome grew to a height of about 250 meters above the vent. Assuming that the density of dome magmas was  $1600 \text{ kg m}^{-3}$  [Olhoeft et al., 1981], the exit pressure at the vent increased by about 4 MPa. This represents a significant change of pressure, with implications for degassing and the gas content of ascending magma.

### 2. Pressure and Gas Content in the Magma Column Below the Vent

[5] The volatile content of MSH magma is about 5 wt% [Rutherford et al., 1985], implying a very large volume fraction of gas at the atmospheric pressure if exsolution and expansion proceed in a closed system. The transition from explosive to effusive eruption regimes reflects the increasing importance of gas leakage from rising magma as the eruption rate decreases [Eichelberger et al., 1986; Jaupart and Allègre, 1991]. Hydrogen isotopic systematics are indeed consistent with open system degassing [Anderson and Fink, 1989].

<sup>1</sup>Equipe de Dynamique des Fluides Géologiques, Institut de Physique du Globe de Paris, Paris, France.

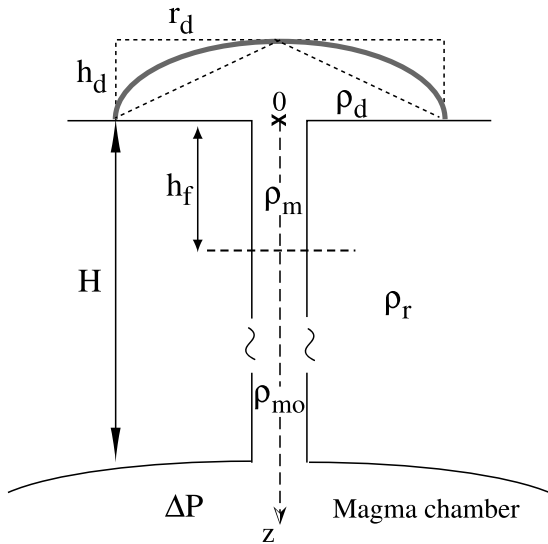


**Figure 1.** Model set-up. A dome with radius  $r_d$  and thickness  $h_d$  generates compressive stresses around the volcanic conduit. A magma column extends from a reservoir at depth  $H$  to a vent beneath the dome. Fractures around the conduit are closed down to depth  $h_f$ . Short-dashed lines illustrate the two limiting dome shapes used to calculate induced stresses: a flat disk and a cone.

[6] We invoke two key principles. One is that gas leakage must initially be efficient at very shallow levels because of the large changes of solubility that occur at small pressures. For example, assuming equilibrium conditions, magma that is saturated with water at a pressure of only 0.4 MPa, corresponding to a depth of only 10 m, would contain 95% gas by volume at the atmospheric pressure. The other principle is that a lava dome acts to increase pressures in the magma column and in rocks surrounding the conduit. At MSH, crucial observations are that the dome height kept on increasing with each successive phase and that each growth phase ended as magma ascent ceased. Thus, growth proceeded until the magma column was in hydrostatic equilibrium with the reservoir. A growth increment requires a new hydrostatic equilibrium state, which can be achieved by lowering density values in the magma column. The composition and initial volatile content of the MSH magma did not vary appreciably and hence the only way to change magma density is to modify the gas content.

[7] Loading of the crater floor by the dome acts to increase pressure in rocks surrounding the conduit and to close fractures along the conduit walls (Figure 1). This effect is only significant down to some depth  $h_f$ . To estimate this depth, we use solutions given by *Pinel and Jaupart* [2000] for stresses generated by a lava dome. The crater floor and basement deform in an elastic regime. The dome is axisymmetric with height  $h_d$  and radius  $r_d$  and its average density is  $\rho_d$ . A lava dome thins away from its axis and has

steep outerflanks, and we have considered two different shapes to bracket the true one: a cone and a flat disk. The induced normal stress is a function of dimensionless depth  $z^* = z/r_d$  in the axial region. It takes the same value at  $z = 0$  for both dome shapes and becomes negligible at  $z/r_d \approx 1$  for the cone and  $z/r_d \approx 1.5$  for the disk. Closure of fractures along the conduit walls depends on the applied pressure and on the fracture size. In the deformed cores of major crustal faults, permeability decreases with increasing effective normal stress  $\sigma$  according to  $k = k_o \exp(-\sigma/\sigma^*)$ , where constant  $\sigma^*$  may be as small as 2.5 MPa [*Rice, 1992*]. This shows that the permeability of highly cracked rocks is sensitive to small stress changes. Furthermore,  $\sigma^*$  decreases as  $k_o$  increases, and one expects very large permeability values in a shallow volcanic environment [*Jaupart and Allègre, 1991; Diller et al., 2006*]. A fracture of length  $l$  and aperture  $\delta$  gets closed by a pressure increase of  $\approx G \delta/l$ , where  $G$  is rigidity. From field observations, typical values for the length and width of actively degassing fractures connected to a conduit wall are 10 m and 1 mm, respectively [*Stasiuk et al., 1996*]. For  $G = 10^9$  Pa, the overpressure required for closure is only 0.1 MPa in this case. Fractures that extend to the surface are obviously longer than this example and are even more sensitive to pressure. Thus, degassing paths can be shut down by very small pressure changes and we assume that this is effective as long as stresses induced by the dome remain significant, *i.e.* down to a depth which is between  $r_d$  and  $1.5 r_d$ . We shall consider that  $h_f = \alpha r_d$ , where  $\alpha$  is some constant.  $\alpha$  is expected to lie in the 1–1.5 range and will be adjusted to fit the data.

[8] We calculate pressures at the end of a dome-building episode, when the magma column is in hydrostatic equilibrium. Below depth  $h_f$ , magma leaks all its gas and we assume that its density is constant and equal to  $\rho_{mo}$ . We start from the reservoir located at depth  $H$ , where pressure is equal to the lithostatic value plus an overpressure  $\Delta P$  (Figure 1). Thus, the magma pressure at  $z = h_f$  is:

$$P(h_f) = P_{litho}(H) + \Delta P - \rho_{mo}g(H - h_f) \quad (1)$$

Between  $z = h_f$  and  $z = 0$ , we assume that magma does not lose any gas (closed system behaviour) such that its density depends on gas content  $x_g$ . The governing equations are:

$$\frac{dP}{dz} = -\rho_m g \quad (2)$$

$$\frac{1}{\rho_m} = \frac{x_g}{\rho_g} + \frac{1 - x_g}{\rho_{mo}} \quad (3)$$

$$x_g \approx x[P(h_f)] - x(P) \quad (4)$$

**Table 1.** Parameters and Physical Properties Used in the Calculation

Parameters	Properties	Symbol	Value
Density of volatile-free magma	$kg m^{-3}$	$\rho_{mo}$	2600
Gas density	$kg m^{-3}$	$\rho_g$	calculated as by <i>Jaupart and Allègre</i> [1991]
Parameter of the solubility law	$Pa^{-1/2}$	$s$	$4.11 \cdot 10^{-6}$

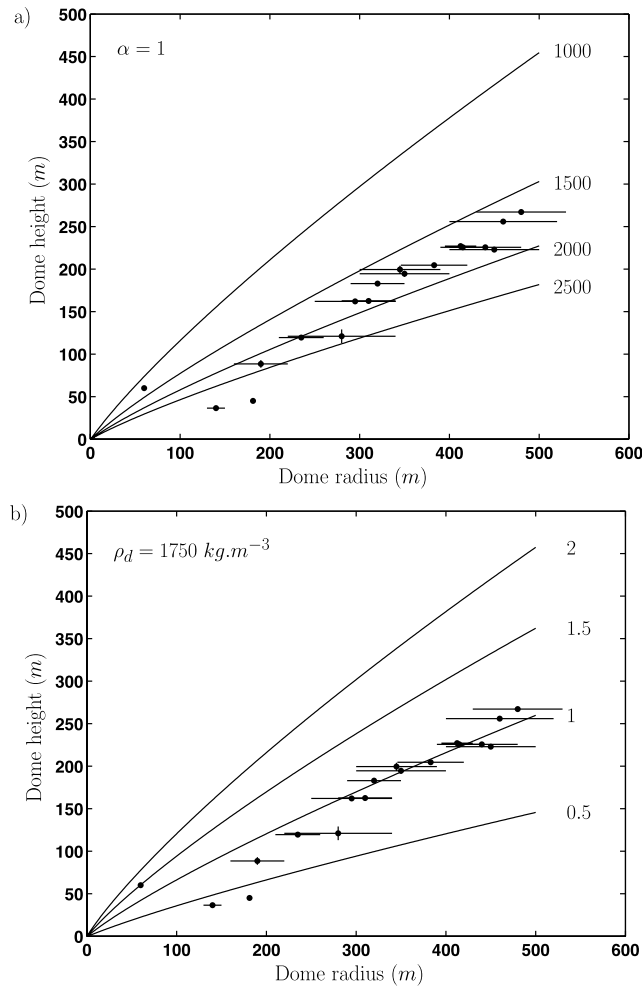


**Figure 2.** Calculated dome thickness as a function of dome radius. Horizontal error bars correspond to the minimum and maximum width estimates. Data from Swanson *et al.* [1987] and Swanson and Holcomb [1990]. (a) Fixed  $\alpha = 1$  (such that  $h_f = \alpha r_d$ ) and different average dome densities. (b) Different values of  $\alpha$  and fixed dome density ( $\rho_d = 1750 \text{ kg m}^{-3}$ ).

where  $x(P)$  is the solubility of volatile phases in magma. We choose a simple solubility law of the form  $x(P) = s P^{1/2}$ . Parameters and physical properties are listed in Table 1. We thus calculate  $P_o$ , the pressure at the volcanic vent, i.e. at the base of the dome. This pressure can also be determined from the dome side, such that  $P_o = \rho_d g h_d + P_{atm}$ , where  $\rho_d$  is the average dome density and  $P_{atm}$  is the atmospheric pressure.

[9] Solving the above equations leads to a relationship between the height and radius of the dome. We set the values of  $\rho_r$  and  $\Delta P$  so that  $h_d = 0$  when  $h_f = 0$ . This is justified by the observation that the initial domes stalled when they were very thin ( $\approx 40$  m). Results are shown in Figure 2 for various values of  $\rho_d$  and  $\alpha$ . This very simple theory predicts a general trend of decreasing height-to-radius ratio which is consistent with the observations. Furthermore, the values of  $\rho_d$  and  $\alpha$  that are required to fit the data are in good agreement with independent constraints.  $\alpha$  must indeed be between values of about 1 and 1.5 and the maximum dome density is about  $2600 \text{ kg m}^{-3}$ ,

which is that of gas-free MSH magma [Olhoeft *et al.*, 1981]. As shown in Figure 2b, a good fit through the data is achieved for  $\alpha = 1$  and  $\rho_d = 1750 \text{ kg m}^{-3}$ , which is very close to the density of June 1980 dome samples [Olhoeft *et al.*, 1981].

### 3. Discussion

#### 3.1. Lateral Versus Vertical Gas Escape

[10] One tenet of the model is that gas loss is more effective in the horizontal direction than along the vertical. Two competing effects are involved. On the one hand, if bubbles deform, permeability is enhanced in the direction of bubble elongation, i.e. along the vertical. On the other hand, magma expansion is laterally constrained by the conduit walls, which acts in favor of horizontal permeability development [Llewellyn, 2007]. For bubbles that remain spherical, gas percolation occurs first in the horizontal direction [Llewellyn, 2007]. Bubble deformation depends on shear stress, which decreases with the eruption rate. Thus, the latter effect is likely to dominate for the small magma velocities that characterize dome-building.

#### 3.2. Long-Term Changes of Dome Properties

[11] Predictions are not in perfect agreement with the data. It would be fruitless to list all the complications that probably come into play and we discuss only one possibility. We have assumed that the average dome density did not change with time and was  $1750 \text{ kg m}^{-3}$ , corresponding to vesicular dacite with about 35% gas bubbles. With time, endogenous growth became more and more important, such that a large fraction of the newly added magma remained within the dome. Such conditions are favorable to gas retention, and it may well be that the average dome density decreased slightly with time. This would explain the slight

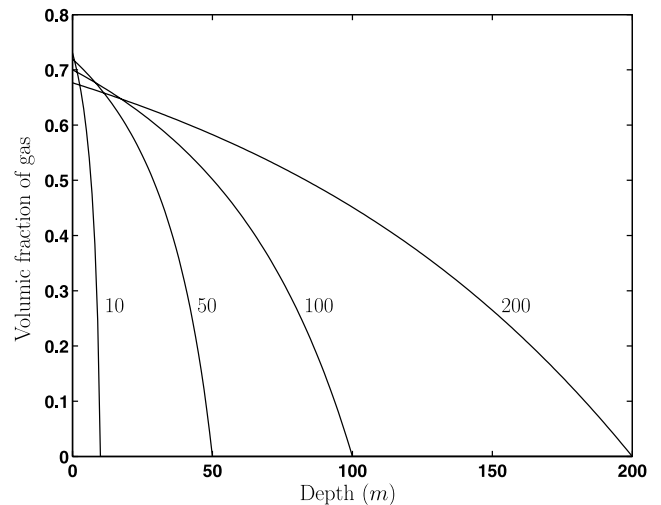


**Figure 3.** Volume fraction of gas in magma as a function of depth beneath the vent for various values of closure depth  $h_f$  (in metres). The vent pressure is determined by the height of the dome (see text). Dome growth has two competing effects on the gas content of magma in the conduit. It inhibits volatile exsolution and gas expansion but also enhances gas retention.

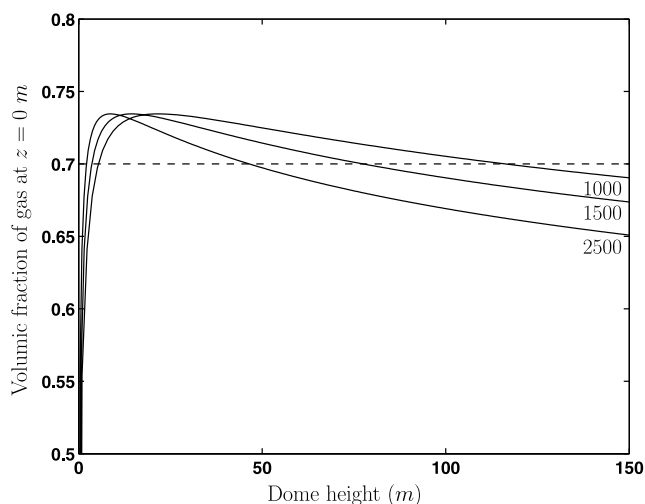


**Figure 4.** Volume fraction of gas in magma at the vent as a function of dome height for various average density values for the dome (in  $\text{kg m}^{-3}$ ). Magma does not lose gas between  $z = 0$  and  $z = h_f$ , due to loading by the dome, as specified in the text. Note that the gas content reaches a maximum for a specific dome height.

offset of the data for early phases when compared to the average predicted trend (Figure 2).

### 3.3. Mechanism of Intermittent Dome Growth

[12] In our model, dome growth stops when hydrostatic equilibrium conditions are restored. A new episode is triggered by the spreading of the dome, a slow process due to the large magma viscosity and the carapace resistance. From the analysis of Huppert [1982], the time-scale for the spreading of a dome of height  $h$  and volume  $V$  is  $\tau = \mu V / \rho_d g h^4$ , where  $\mu$  is the effective dome viscosity. Using the best-fit viscosity value of  $10^{11}$  Pa s obtained for the Soufriere de Saint Vincent dome [Huppert *et al.*, 1982] and representative values of 100 m and  $10^7$  m<sup>3</sup> for  $h$  and  $V$ , this time-scale is about 12 days. At MSH, dome subsidence was observed during each of the 1981–1983 repose periods [Swanson *et al.*, 1987]. For example, it was about 20 m between May 15–21, 1982. Such sagging leads to a magma column that is no longer in hydrostatic equilibrium and hence to magma flow in the conduit. The dome spreads over a larger horizontal distance, and hence the newly ascending magma is prevented from leaking gas over a larger depth extent, allowing a taller magma column above the reservoir.

### 3.4. Dome Stability

[13] The present model involves two competing effects on the gas content of magma in the conduit: an increase of pressure and enhanced gas retention (Figure 3). The gas content of magma at the vent is shown in Figure 4 as a function of dome height. For small dome heights, it increases due to the suppression of leakage channels and the large variations of solubility that occur at small pressures. This suggests that early domes may not be stable: the gas content increases to large values that allow fragmentation. We note that early MSH domes were indeed destroyed by explosions. The first lava dome, which was built in June 12–19, 1980, was partially blown up on July 22 by an

explosive eruption that blasted a crater through its center, indicating that the new magma had fragmented below the vent. Above a certain threshold dome thickness, the gas content at the vent decreases due to the increasing weight of lava and such explosive events are prevented.

## 4. Conclusion

[14] Effusion of degassed lava requires gas leakage beneath the volcanic vent, and hence permeable conduit walls. Loading by a dome acts to close fractures at shallow depth in the edifice and to enhance gas retention in the magma. Thus, dome growth can in fact promote explosive volcanic conditions. One expects different behaviours between domes that are free to spread laterally over large distances and domes that are constrained within the confines of small craters. Our simple model draws attention to the sensitivity of eruption conditions to processes that are active within a few hundred meters of the eruptive vent. It also shows why dome dimensions must be accounted for by eruption models.

[15] **Acknowledgments.** We are grateful to IPGP cont. #2431 for financial support. Careful comments and criticisms by Antonio Costa and an anonymous reviewer led to substantial improvements.

## References

- Anderson, S. W., and J. F. Fink (1989), Hydrogen-isotope evidence for extrusion mechanisms of the Mount St. Helens lava dome, *Nature*, *341*, 521–523.
- Costa, A., O. Melnik, R. S. J. Sparks, and B. Voight (2007), Control of magma flow in dykes on cyclic lava dome extrusion, *Geophys. Res. Lett.*, *34*, L02303, doi:10.1029/2006GL027466.
- Diller, K., A. B. Clarke, B. Voight, and A. Neri (2006), Mechanisms of conduit plug formation: Implications for vulcanian explosions, *Geophys. Res. Lett.*, *33*, L20302, doi:10.1029/2006GL027391.
- Eichelberger, J. C., C. R. Carrigan, H. R. Westrich, and R. H. Price (1986), Non-explosive silicic volcanism, *Nature*, *323*, 598–602.
- Huppert, H. E. (1982), The propagation of two-dimensional and axisymmetric viscous gravity currents over a rigid horizontal surface, *J. Fluid. Mech.*, *121*, 43–58.
- Huppert, H. E., J. B. Shepherd, H. Sigurdsson, and R. S. J. Sparks (1982), On lava dome growth, with application to the 1979 lava extrusion of the Soufriere of St. Vincent, *J. Volcanol. Geotherm. Res.*, *14*, 199–222.
- Iverson, R. M. (1990), Lava domes modeled as brittle shells that enclose pressurized magma, with application to Mount St Helens, in *Lava Flows and Domes: Emplacement Mechanisms and Hazard Implications*, edited by J. H. Fink, pp. 47–69, Springer, New York.
- Jaupart, C., and C. J. Allègre (1991), Gas content, eruption rate and instabilities of eruption regime in silicic volcanoes, *Earth Planet. Sci. Lett.*, *102*, 413–429.
- Llewellyn, E. W. (2007), A numerical model for the development of magma permeability during eruption, *Eos Trans. AGU*, *88*(52), Fall Meet. Suppl., Abstract V11F-04.
- Mathews, S., M. C. Gardeweg, and R. S. J. Sparks (1997), The 1984 to 1996 cyclic activity of Lascar volcano, northern Chile: Cycles of dome growth, dome subsidence, degassing and explosive eruptions, *Bull. Volcanol.*, *59*, 72–82.
- Melnik, O. E., and R. S. J. Sparks (1999), Nonlinear dynamics of lava dome extrusion, *Nature*, *402*, 37–41.
- Melnik, O., and R. S. J. Sparks (2005), Controls on conduit magma flow dynamics during lava dome building eruptions, *J. Geophys. Res.*, *110*, B02209, doi:10.1029/2004JB003183.
- Olhoeft, G. R., R. L. Reynolds, J. D. Friedman, G. R. Johnson, and G. R. Hunt (1981), Physical properties of the June dacite dome, in *The 1980 Eruption of Mount St. Helens, Washington, U.S. Geol. Surv. Prof. Pap.*, *1250*, 549–556.
- Pinel, V., and C. Jaupart (2000), The effect of edifice load on magma ascent beneath a volcano, *Philos. Trans. R. Soc. London, Ser. A*, *358*, 1515–1532.
- Rice, J. R. (1992), Fault stress states, pore pressure distributions, and the weakness of the San Andreas fault, in *Fault Mechanics and Transport Properties of Rocks*, edited by B. Evans and T. F. Wong, pp. 475–503, Academic, London.

- Rutherford, M. J., H. Sigurdsson, S. Carey, and A. Davis (1985), The May 18, 1980, eruption of Mount St. Helens: 1. Melt composition and experimental phase equilibria, *J. Geophys. Res.*, *90*, 2929–2947.
- Stasiuk, M. V., C. Jaupart, and R. S. J. Sparks (1993), On the variations of flow rate in non-explosive lava eruptions, *Earth Planet. Sci. Lett.*, *114*, 505–516.
- Stasiuk, M. V., J. Barclay, M. R. Carroll, C. Jaupart, J. C. Ratte, R. S. J. Sparks, and S. R. Tait (1996), Degassing during magma ascent in the Mule Creek vent (USA), *Bull. Volcanol.*, *58*, 117–130.
- Swanson, D. A., and R. T. Holcomb (1990), Regularities in growth of the Mount St. Helens dacite dome, 1980–1986, in *Lava Flows and Domes: Emplacement Mechanisms and Hazard Implications*, edited by J. H. Fink, pp. 3–24, Springer, New York.
- Swanson, D. A., D. Dzurisin, R. T. Holcomb, E. Y. Iwatsubo, W. W. Chadwick, T. J. Casadevall, J. W. Ewert, and C. C. Heliker (1987), Growth of the lava dome at Mount St. Helens, Washington (USA), 1981–1983, *Geol. Soc. Am. Spec. Pap.*, *212*.
- 
- C. Jaupart and B. Taisne, Dynamique des Fluides Géologiques, Institut de Physique du Globe de Paris, 4, place Jussieu, F-75252 Paris CEDEX 05, France. (taisne@ipgg.jussieu.fr)